Nanostructural Cell Wall Changes Due to Thermal Degradation in Wood

Nayomi Z. Plaza[1], Laura E. Hasburgh[1](✉), Lin Yang[2], and Nathan J. Bechle[1]

[1] US Forest Products Laboratory, Madison, Wisconsin, USA
laura.e.hasburgh@usda.gov
[2] Brookhaven National Laboratory, Upton, New York, USA

Abstract. Pyrolysis of wood involves the thermal degradation of the wood polymers and the formation of char. Understanding how char forms, particularly, in terms of the nano-structural changes that take place during pyrolysis will inform fire models to ensure fire safety in timber structures. Here, small- and wide-angle x-ray scattering (SAXS/WAXS) based tomography were used to study how thermal degradation changes wood nanostructure across the pyrolysis zone in Douglas-fir. The changes in the aggregation of cellulose elementary fibrils (via SAXS) as well as changes in the cellulose crystallinity (via WAXS) were measured. Tomographic reconstructions from the scattering contrast and absorption data were computed to visualize and quantify these changes across the entire cellular structure of the samples. Preliminary results revealed relatively abrupt changes in the cellulose crystallinity as the wood polymers are thermally degraded. With SAXS we observed changes in the overall intensity as a function of thermal degradation, which suggests that the packing of the elementary fibrils may be modified as some of the polymers are degraded.

Keywords: pyrolysis · cellulose crystallinity · x-ray scattering

1 Introduction

Despite its wide use in construction, wood's structural integrity is susceptible when it is exposed to elevated levels of moisture, decaying organisms, or temperatures. Understanding how wood changes after being exposed to high temperatures is particularly important to predict and model the fire performance of wood structures [1, 2]. Fire growth models are used to predict the behavior of a fire and rely on various input parameters, including material properties when exposed to high temperatures. However, there is a lack of characterization techniques that allow the study of wood-fire interactions in situ to quantify the changes in material properties more thoroughly in wood during and after exposure to fire.

L. Makovická Osvaldová et al. (Eds.): WFS 2024, *Wood & Fire Safety 2024*, pp. 3–10, 2024.
https://doi.org/10.1007/978-3-031-59177-8_1

1.1 Wood Pyrolysis

When wood is exposed to high temperatures it undergoes pyrolysis, or thermal degradation. As a series of complex chemical and physical changes take place, volatiles are released, and char is formed. Char acts as an insulating layer and is defined as the solid, carbonaceous material that remains and, for engineering analysis, a temperature of 300°C is often used as the temperature for when wood is converted to char [3]. Despite simplification to a finite temperature, a gradient of material properties exists as the three main polymeric components (hemicellulose, cellulose, and lignin) degrade. This gradient includes a pyrolysis zone, which is the zone just beneath the char that has been exposed to high temperatures.

Pyrolysis begins with dehydration at temperatures between 105°C and 200°C [4]. It is widely accepted that the breakdown of the major polymeric components of wood begins at temperatures above 200°C [5]. Hemicelluloses are the least thermally stable and breakdown at lower temperatures between 200 and 260°C. Cellulose thermally decomposes between 240 and 350°C, and lignin thermally decomposes between 280 and 500°C. Even though pyrolysis plays a key role in the combustion of wood, a majority of what we know regarding pyrolysis kinetics is based on the thermogravimetric data from extracted, representative polymers [6]. Our understanding of the nano- and molecular-scale changes within the pyrolysis zone is limited and, due to the variability and the difficulty in obtaining material properties at high temperatures or while undergoing active combustion, many pyrolysis and fire growth models are simplified.

Wood density is the common material property that affects pyrolysis, combustion rates, and decomposition products. However, it is extremely variable between wood species and can even vary within a cross-section of a single tree, and as a function of local temperature. Some models simplify this by using a constant that is representative of the wood, a linear function in the pyrolysis region bound by the char and virgin wood values, or the bulk density of specific condensed phase species (i.e., wet wood, dry wood, char, ash). In our previous work, we used x-ray computerized tomography (XCT) and neutron imaging (NI) to measure densities across pyrolysis zones of partially charred word and found that the density decreased by over 50% from the virgin wood to char [7]. We also observed spatial variations in the density, which could be caused by local changes in the cell wall nanostructure such as the distribution of cellulose microfibrils inside the cell walls or the packing of the elementary fibrils in the microfibrils.

Hence, to better understand the nanostructural changes that may be associated to this gradual density change across the pyrolysis zone, we used simultaneous wide-angle x-ray scattering (WAXS) and small angle x-ray scattering (SAXS) to measure partially charred wood slivers. These techniques have been used previously to measure moisture-induced changes from atomic to nano scales [8, 9] but have yet to be used to study partially charred wood. Changes in the elementary fibril spacing inside microfibrils are accessible via SAXS whereas changes in the cellulose crystalline structure can be studied via WAXS. Moreover, recent advances in x-ray scattering have also enabled new scattering-based imaging techniques [10] that can allow us to visualize changes in the cellular cross-section of wood slivers. By combining these techniques, we have probed changes across the pyrolysis zone from sub-nm to cell wall level. Our preliminary

analysis has shown changes between unmodified wood and char, particularly in terms of the cellulose crystallinity as well as microfibril size and distribution in the cell walls.

2 Methods and Materials

2.1 Wood Specimens

Wood Slivers. A block of Douglas-fir (*Pseudotsuga menziesii*) was cut into approximately 40mm x 1.5mm slices. From the slices, 1.5 mm square slivers were cut that included both early and late-wood.

The wood slivers were taped together using heat-resistant tape along the bottom edge to recreate an uncut slice. On the middle slice, three duplex 30 AWG (0.25 mm diameter) Type K thermocouples, insulated with Kapton®, PFA, Glass Braid Insulation (Omega Engineering, GG-K-30-SLE) were installed at 5, 10, and 25 mm from the exposed top surface. To reduce the bulk and allow the slices to be tightly held together without extra gaps, the glass braid was removed from the portion of the thermocouple that was sandwiched between slices. An additional thermocouple was also placed at 25 mm from the exposed surface to determine when to terminate the exposure (Fig. 1).

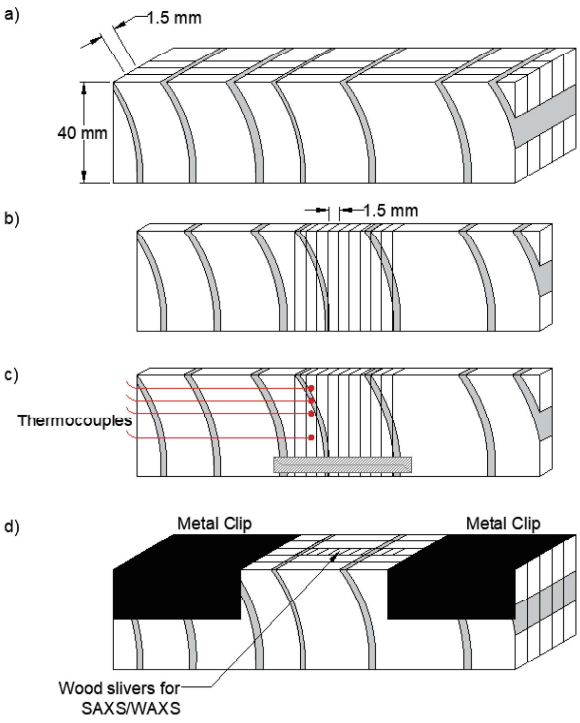

Fig. 1. Schematic of specimen development process with a) wood block cut into 1.5 mm thick slices, b) one slice further cut into slivers, c) heat-resistance tape and thermocouple placement, and d) specimen sandwich.

Thermal Gradient in Wood. The wood specimens were placed in a standard cone calorimeter specimen holder with frame and packed on each side with ceramic batting such that only the top surface was exposed to a heat flux (Figure 2).

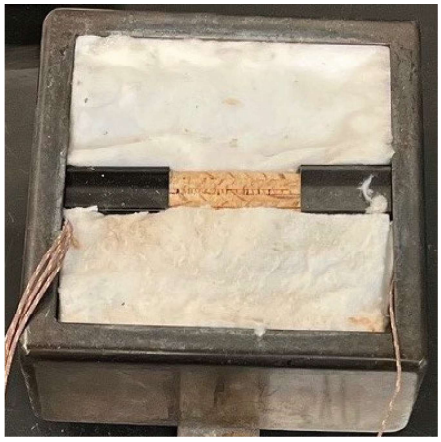

Fig. 2. Specimen loaded in standard cone calorimeter specimen holder with frame.

The specimen was then exposed to a constant radiant heat flux of 30 kW/m^2 using a conical heater from a cone calorimeter (FTT iCone Mini, East Grinstead, West Sussex, UK). The spark ignitor was not used, and the tests were terminated when the thermocouple located at 25mm reached 100°C by removing the specimen and spraying water on it. Table 1 provides the approximate final temperature profile for the charred wood slivers used for the SAXS/WAXS and tomography experiments.

Table 1. Thermocouple temperatures at end of exposure

Distance from Exposed Surface [mm]	Temperature [°C]
5	493.7
10	366.7
25	103.3

2.2 SAXS/WAXS and Tomography

Small angle x-ray scattering (SAXS), wide-angle X-ray scattering (WAXS) and scattering contrast-based tomography experiments were performed on the 16ID-LIX Beamline at the National Synchrotron Light Source II at the Brookhaven National Laboratory (Upton, New York) using the micro-beam structural mapping configuration [11]. Partially charred wood slivers were mounted on a threaded standoff that was fastened onto a

3D printed kinematic mount available at the beamline (see Figure 3). The X-ray energy was 5 keV, and the spot size was approximately 5 microns. Data were collected using two Pilatus detectors to achieve a combined q-range of 0.006-2.8 $Å^{-1}$. Here, q is the scattering vector and is defined as $q = 4\pi/\lambda \sin(\theta)$, λ is the x-ray wavelength and θ is ½ of the scattering angle. Tomographic data was acquired at nine different locations along the sample height, ranging from 3 to 13 mm with respect to the exposed surface. Reconstruction was performed using tomopy [12]. Additionally, we also obtained 2D scans at three different projection angles with respect to the x-ray beam. Data were visualized, processed, and reduced from 2D maps to 1D scattering profiles using the python libraries py4xs and lixtools [13].

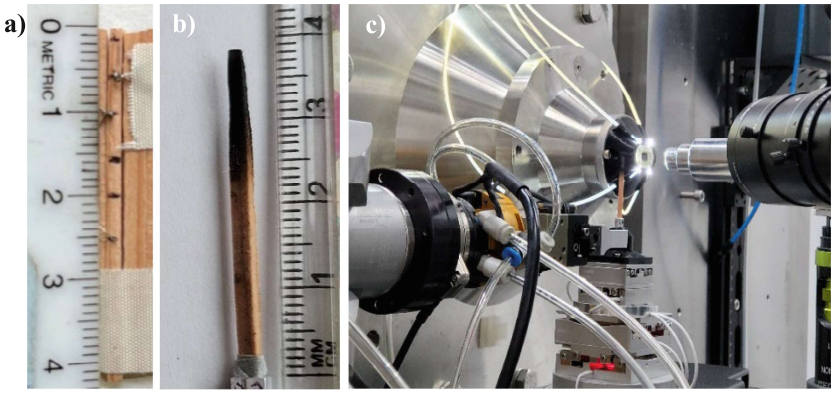

Fig. 3. Photographs showing a) uncharred specimen with thermocouple locations secured via thermal tape, b) charred specimen within kinematic mount used for SAXS/WAXS experiments, and c) specimen in LiX beamline at Brookhaven National Laboratory.

3 Results and Discussion

Tomographic reconstructions from the scattering contrast data were computed to visualize and quantify these changes across the entire cellular structure of the samples [11]. Figure 4a shows a representative intensity profile computed by azimuthal averaging assuming the underlying fiber geometries are aligned with the rotation axis. The intensities around the peak observed at $q=1.6$ $Å^{-1}$ correspond to the 200 cellulose Iβ diffraction peak and were chosen to track the crystalline cellulose component, while the intensities around the valley at $q=1.3$ $Å^{-1}$ were assumed to characterize the abundance of amorphous non-cellulose crystalline material (shaded as blue and green, respectively in Figure 4a). Tomographic reconstructions (Figure 4b) were computed using these intensity classifications via *tomopy* [12]. We also calculated the cellulose to amorphous ratio of the reconstructed regions labeled below as crystallinity index. Preliminary results revealed relatively abrupt changes in the cellulose crystallinity as the wood polymers are thermally degraded. This can be observed in the differences between the tomograms for slices at exposed distances of 13mm (assumed to be uncharred wood) and 11mm

(within the pyrolysis zone). Similar changes were also observed in the x-ray absorption as some mass is lost due to thermal degradation and the associated local sample density decreases.

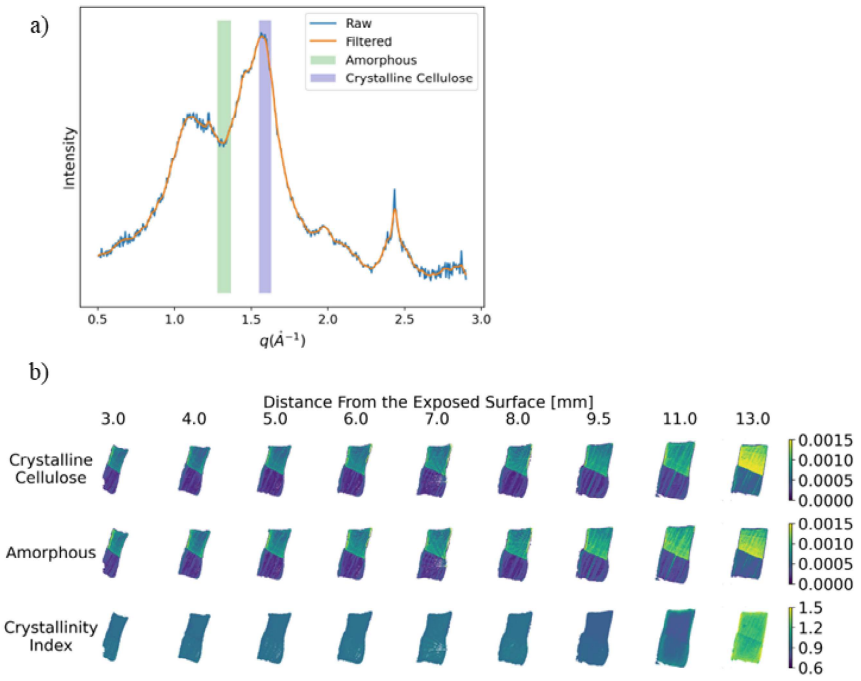

Fig. 4. X-ray scattering results for Douglas fir specimen with a) representative 1D intensity profile of azimuthal averaged profiles displaying the intensity regions used to calculate the crystalline index (i.e. crystalline cellulose and amorphous (non-crystalline); and b) tomographic reconstructions at various distances from the exposed surface using the scattering intensities from cellulose and amorphous polymers as well as the crystallinity index, which is the ratio of crystalline cellulose to amorphous scattering intensities.

To better understand the structural changes taking place across the pyrolysis zone, a majority of the discolored zone was scanned (see Figure 5a) to obtain a 2D intensity map of the scattering data (Figure 5b). SAXS/WAXS intensity profiles were then obtained at different locations ranging from unmodified to charred zones are shown in Figure 5C. There are differences between scattering from the unmodified wood and the charred region in both the WAXS ($q > 0.8$ Å^{-1}) and the SAXS regimes ($q < 0.5$ Å^{-1}). As expected, in the WAXS region we observe the diffraction peaks characteristic of cellulose, (i.e. 200, 004 and the 101 and 1-10). These peaks become less intense in measurements obtained closer to the char (below 10.5 mm), and eventually disappear (~5 mm). Measurements taken closer to the char exhibit a broader peak towards the right of the cellulose Iβ 200 peak (q~1.56 Å^{-1}) and no other diffraction peaks. Scattering from the cellulose elementary fibrils and their bundles contribute to the shoulder observed in the SAXS

regime (q ~0.08 $Å^{-1}$). This shoulder becomes less broad and shifts towards lower q as the distance to the charred surface decreases. This low-q shoulder is not visible in measurements taken near the charred surface; however, we observe a new mid-q broad peak that increases in intensity and shifts towards lower-q near the charred end. The disappearance of the characteristic signals from the scattering of wood suggests that as the wood polymers thermally degrade, they first lose crystallinity. The changes in the SAXS regime also suggest the microfibril size, packing and/or distribution in the cell wall was affected by the thermal degradation. Further analysis to deconvolute these contributions and quantify the crystallinity index and elementary fibril spacing across the pyrolysis zone is underway.

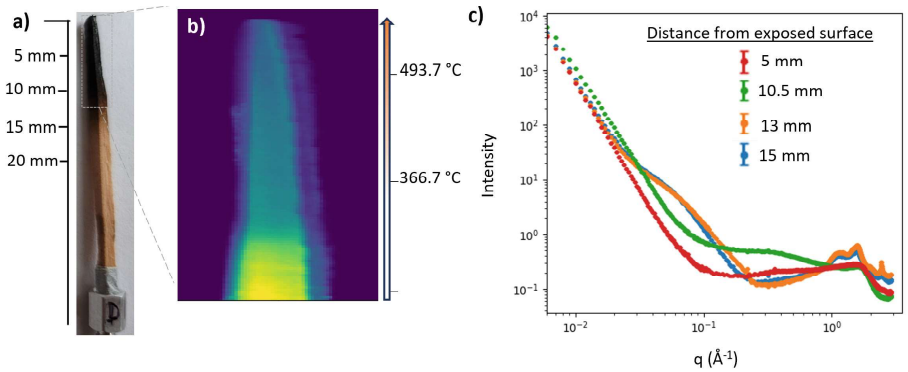

Fig. 5. SAXS-WAXS data for Douglas Fir charred wood sliver. (a) Mounted specimen, and the area mapped using SAXS-WAXS scanning is shown in dashed lined (which ranged from 3 mm to 15 mm from the exposed surface). (b) Corresponding 2D scattering intensity map for the probed area. (c) SAXS-WAXS 1D intensity profiles as a function of location with respect to the exposed surface from the (b) 2D map.

4 Conclusions

Here, we explored the use of simultaneous SAXS-WAXS and scattering-based tomography to characterize the nanostructural and cellular changes that occur along the pyrolysis zone of a partially charred wood sliver. The method developed in this work allowed us to prepare intact wood slivers with a thermally degraded gradient along their height and whose dimensions and fiber orientation was suitable for the x-ray scattering analysis. Qualitative assessments of the intensity profiles have shown that thermal degradation of the wood sliver resulted in a reduction of the cellulose crystallinity as well as a changes in the SAXS regime that suggest the wood polymer degradation might be modifying the cellulose microfibril size and distribution in the cell wall. Despite the decreasing contribution of these characteristic signals, we were still able to use the scattering contrast to reconstruct the tomographic data and visualize the changes in the transverse plane without needing to section the samples. Shrinkage in the transverse plane was noticeable throughout the pyrolysis zone.

Acknowledgments. The authors would like to acknowledge the use of 16ID-LiX at NSLS thru awarded beamtime (GUP-#312267). The LiX beamline, which is part of the Center for Biomolecular Structure (CBMS), which is primarily supported by the NIH National Institute of General Medical Sciences (NIGMS) through a P30 Grant (P30GM133893) and by the DOE Office of Biological and Environmental Research (KP1605010). LiX is also supported with NIH Grant S10 OD012331. As part of NSLS-II, a national user facility at Brookhaven National Laboratory, work performed at the CBMS is supported in part by the DOE Office of Science, Office of Basic Energy Sciences Program under contract number DE-SC0012704.

References

1. Lautenberger, C.: A generalized pyrolysis model for combustible solids (PhD. Thesis). University of California - Berkeley (2007)
2. Yang, F., Rippe, C., Hodges, J., Lattimer, B.: Methodology for material property determination. Fire Mater. **43**(6), 694–706 (2019)
3. White, R.H.: Analytical methods for determining fire resistance of timber members. In: Hurley, M.J., et al. (eds.) SFPE Handbook of Fire Protection Engineering, pp. 1979–2011. Springer, New York (2016). https://doi.org/10.1007/978-1-4939-2565-0_55
4. Hill, C.A.: Wood Modification: Chemical, Thermal and Other Processes. John Wiley & Sons, Hoboken (2007)
5. Shafizadeh, F., Chin, P.P.: Thermal deterioration of wood. Wood Technol.: Chem. Aspects **43**, 57–81 (1977)
6. Hasburgh, L.E., Stone, D.S., Zelinka, S.L., Plaza, N.Z.: Characterization of wood chemical changes caused by pyrolysis during flaming combustion using x-ray photoelectron spectroscopy. In: Makovicka, L. Markert, F., Zelinka, S.L. (eds.) Wood & Fire Safety: Proceedings of the 9th International Conference on Wood & Fire Safety, pp. 22-27. Springer International Publishing, Slovakia (2020). https://doi.org/10.1007/978-3-030-41235-7_4
7. Hasburgh, L.E, Bechle, N.J, Plaza, N.Z: Two proof-of-concept, nontraditional density measurement techniques for partially charred wood. In: Symposium on Obtaining Data for Fire Growth Models, pp. 97-107. ASTM International (2023)
8. Arzola-Villegas, X., Lakes, R., Plaza, N.Z., Jakes, J.E.: Wood moisture-induced swelling at the cellular scale-Ab intra. Forests **10**(11), 996 (2019)
9. Penttilä, P.A., et al.: Moisture-related changes in the nanostructure of woods studied with X-ray and neutron scattering. Cellulose **27**(1), 71–87 (2020)
10. Omori, N.E., Bobitan, A.D., Vamvakeros, A., Beale, A.M., Jacques, S.D.: Recent developments in X-ray diffraction/scattering computed tomography for materials science. Phil. Trans. R. Soc. A. **381**, 20220350 (2023)
11. Yang, L., Liu, J., Chodankar, S., Antonelli, S., DiFabio, J.: Scanning structural mapping at the life science x-ray scattering beamline. J. Synchrotron Radiat. **29**, 540–548 (2022)
12. Gürsoy, D., De Carlo, F., Xiao, X., Jacobsen, C.: TomoPy: a framework for the analysis of synchrotron tomographic data. J. Synchrotron Radiat. **21**(5), 1188–1193 (2014)
13. Yang, L.: NSLS-II-LIX: Lixtools. GitHub (2023). https://github.com/NSLS-II-LIX/lixtools